Power Sources

DOI: 10.1002/ange.200601301

Novel Nanocomposite Pt/$RuO_2 \cdot x H_2O$/Carbon Nanotube Catalysts for Direct Methanol Fuel Cells**

*Lin Cao, Frieder Scheiba, Christina Roth, Franz Schweiger, Carsten Cremers, Ulrich Stimming, Hartmut Fuess, Liquan Chen, Wentao Zhu, and Xinping Qiu**

Two key problems inhibiting the commercialization of direct methanol fuel cells (DMFCs) are the cost of the precious metals employed and the sluggish kinetics and catalyst poisoning by CO or CHO species. Research to solve the first drawback[1–4] focuses on the reduction of precious metal loading, which is achieved by increasing the catalyst's specific surface area and its accessibility. For the second problem, advanced electrocatalyst design relies on the "bifunctional approach",[5–10] in which a second compound such as ruthenium or $RuO_2 \cdot x H_2O$ assists the oxidation of CO or CHO species by adsorption of oxygen-containing species close to the poisoned Pt sites. In contrast to previous work on PtRu alloy catalysts,[11–13] Rolison and co-workers[14,15] emphasized the importance of hydrous ruthenium oxides because the $RuO_2 \cdot x H_2O$ speciation of Ru in nanoscale PtRu blacks shows both high electron and proton conductivity, which results in a much more active catalyst for methanol oxidation. However, direct evidence of the catalytic function of hydrous oxides is very scarce.

Mixed proton–electron conducting materials should be ideal catalyst supports for DMFCs since they allow for low ohmic resistance in both the proton and electron conduction at the same time. As hydrous ruthenium(IV) oxide has been reported to contain liquid or liquid-like regions of water to

[*] Dr. L. Cao, Prof. L. Chen, Prof. W. Zhu, Prof. Dr. X. Qiu
Key Lab of Organic Optoelectronics and Molecular Engineering
Department of Chemistry
Tsinghua University
Beijing, 100084 (P.R. China)
Fax: (+86) 6279-4235
E-mail: qiuxp@mail.tsinghua.edu.cn

F. Scheiba, Dr. C. Roth, Prof. Dr. H. Fuess
Institut für Materialwissenschaften
Technische Universität Darmstadt
64287 Darmstadt (Germany)

F. Schweiger, Dr. C. Cremers, Prof. Dr. U. Stimming
Abteilung 1: Technik für Energiesysteme und erneuerbare Energien
Bayerisches Zentrum für Angewandte Energieforschung (ZAE)
85748 Garching (Germany)

[**] We are grateful for financial support from the Sino-German Center (GZ 218 (101/6)), the State Key Basic Research Program of the People's Republic of China (2002CB211803), the National Natural Science Foundation of China (90410002), and the Deutsche Forschungsgemeinschaft (Fu 125/41-1 and Sti 74/17).

Supporting Information for this article is available on the WWW under http://www.angewandte.org or from the author.

facilitate proton conduction within an electron-conducting matrix,[16] it appears to be a promising material. To facilitate mass transport in liquid-feed operation and within the mostly thicker electrodes in DMFCs, carbon nanotubes (CNTs) have been chosen as a new support type. CNTs form a porous nanotube micronetwork and therefore show highly electrochemically accessible surface areas. Furthermore, they offer an outstanding electronic conductivity relative to the commonly used Vulcan carbon blacks. A schematic diagram of a novel catalyst design based on the above is given in Scheme 1.

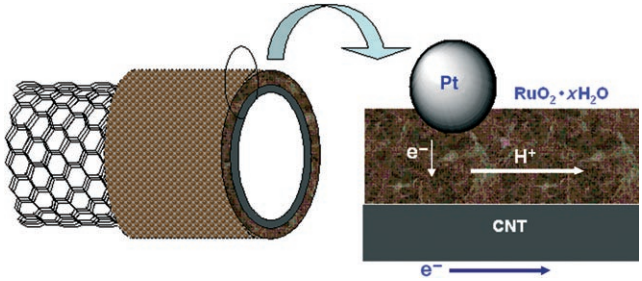

Scheme 1. Schematic diagram of the novel catalyst.

Herein, we describe a composite catalyst combining the properties of hydrous ruthenium oxide in contact with a Pt phase and a new type of carbon support. This novel catalyst design takes into account the problems of CO poisoning, high precious metal loading, and insufficient mass transport in thick electrode layers. The obtained catalyst with 14.8 wt % Pt loading on the support and a Pt:Ru ratio of 1:1 shows superb performance for direct electrooxidation of methanol.

The novel materials were prepared by purifying and pretreating commercial carbon nanotubes (Tsinghua University) in 1 % sodium dodecyl sulfate (SDS) to increase their hydrophilicity. The $RuO_2{\cdot}x\,H_2O$ coating was obtained by an oxidant-aided co-precipitation technique. The procedure for preparing nanocomposite $Pt/RuO_2{\cdot}x\,H_2O$/CNT and details of the electrochemical measurements are described in the Experimental Section. Figure 1 shows transmission electron micrographs of platinum nanoparticles decorated on hydrous ruthenium oxide coated SDS-treated carbon nanotubes. As shown in Figure 1 a, the carbon nanotubes exhibit a multiwalled microstructure with an average diameter of about 40 nm. More importantly, however, very high particle densities for platinum and/or $RuO_2{\cdot}0.56\,H_2O$ were found at all CNT surfaces in the image. Consequently, the surfactant-aided sonication applied for the dispersion of the CNTs combined with the chosen deposition method appears to be a very powerful and effective technique.

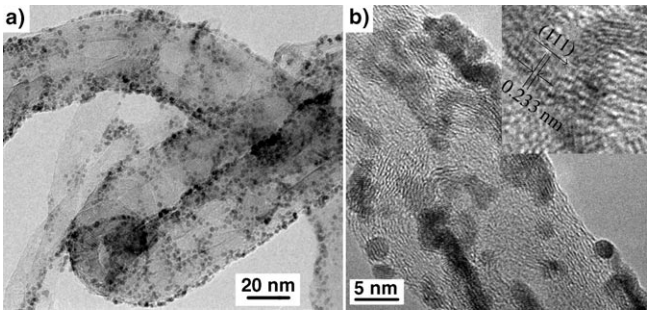

Figure 1. Transmission electron micrographs of $PtRuO_2{\cdot}0.56\,H_2O$/CNT: a) the multiwalled structure of the carbon nanotubes can be seen in this low-resolution image, with nanoparticles highly dispersed on the tube surface; b) nanoparticles (average diameter of 2.4 nm) show visible lattice planes; from the high-resolution inset a lattice spacing *d* of 0.233 nm can be determined.

The hollow structure of the CNTs (as reported in numerous publications) is not clearly visible from Figure 1 b, probably to the $RuO_2{\cdot}0.56\,H_2O$ coating. According to the high-resolution TEM image (inset in Figure 1 b) the distance between two adjacent lattice planes (indicated by the *d* spacer in the image) is approximately 0.233 nm. This length is attributed to Pt(111) and is consistent with the results obtained from X-ray diffraction (see the Supporting Information). The average platinum particle size was determined from the TEM images to be about 2.4 nm, which is in the range of, or even smaller than, that reported by other authors.[17] Despite the small size of the platinum particles, particle agglomeration is very rare, probably because of the large number of nucleation centers available on the surface of the $RuO_2{\cdot}0.56\,H_2O$ coated CNTs. This unique structure appears to provide a suitable support for many uniform platinum particles, thereby favoring the high performance of methanol oxidation, as discussed below.

The $Pt/RuO_2{\cdot}0.56\,H_2O$/CNT samples were tested for their activity in the electrooxidation of methanol. To investigate the role played by the $RuO_2{\cdot}0.56\,H_2O$ coating further, a Pt/CNT catalyst with the same Pt-to-CNT ratio was prepared for comparison. In addition, experiments with a carbon-supported binary PtRu catalyst (E-TEK; 20 wt % on Vulcan, Pt:Ru = 1:1) and a carbon-supported Pt catalyst (E-TEK; 20 wt % on Vulcan) were carried out for comparison. Figure 2 shows voltammetric curves recorded for the synthesized and reference catalysts in 1 M CH_3OH + 1 M $HClO_4$ as supporting electrolyte. $Pt/RuO_2{\cdot}0.56\,H_2O$/CNT displays a 1.5-times higher current density than the PtRu/Vulcan catalyst. Considering that the as-prepared catalyst and PtRu/Vulcan have almost identical Pt loadings, $Pt/RuO_2{\cdot}0.56\,H_2O$/CNT appears to be significantly more active for methanol oxidation. Furthermore, the onset and peak potentials of $Pt/RuO_2{\cdot}0.56\,H_2O$/CNT are both lower than those of PtRu/Vulcan, thus indicating a high availability of hydroxide species adsorbed on the surface in the proximity of the active platinum sites that promote the methanol oxidation. Apart from a slight shift to higher potentials for the Vulcan-supported catalyst, the cyclic voltammograms (CVs) of Pt/CNTs and Pt/Vulcan appear almost identical, thus indicating that the promoting effect of the $Pt/RuO_2{\cdot}0.56\,H_2O$/CNT catalyst is mainly due to the $RuO_2{\cdot}0.56\,H_2O$ coating on the tubes.

We further hypothesized that the $RuO_2{\cdot}0.56\,H_2O$ coating can promote methanol oxidation. Indeed, another piece of evidence to support such a bifunctional mechanism is shown in Figure 3. To obtain further insight into the role played by ruthenium and ruthenium oxide in the catalysts, the CV curves of different scanning cycles of the PtRu/Vulcan

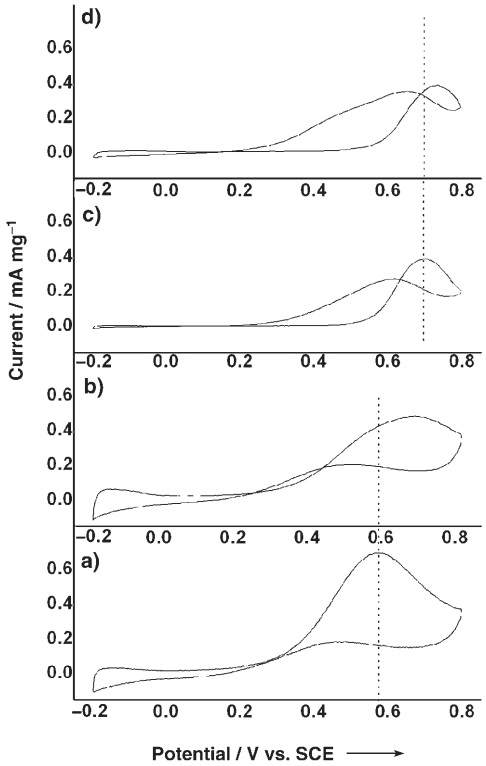

Figure 2. Cyclic voltammograms for Pt/RuO_2·0.56H_2O/CNT (a), PtRu/Vulcan (b), Pt/CNT (c), and Pt/Vulcan (d). See the Experimental Section for further details.

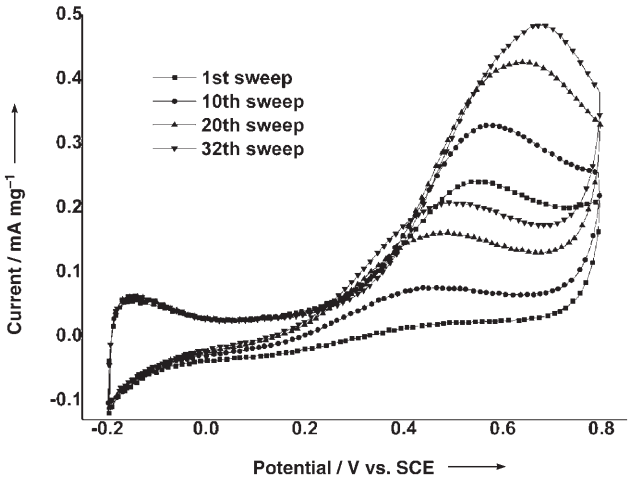

Figure 3. Cyclic voltammograms of different scanning cycles of the PtRu/Vulcan electrode at 25 °C in 1 M CH_3OH + 1 M $HClO_4$ in the potential range −0.2 to 0.8 V vs. SCE with a scan rate of 50 mVs^{-1}.

electrode were recorded. The CV curve for the first cycle shows a rather low methanol oxidation current. High activities are only obtained after 32 sweeps, which can be considered to be due to a kind of electrochemical activation in order to form ruthenium oxide. However, in the case of Pt/RuO_2·0.56H_2O/CNT, only eight scanning cycles are needed for a significant activation. This implies that the PtRu/Vulcan catalyst needs a longer induction period than PtRuO_2·0.56H_2O/CNT to show a good performance for methanol oxidation.

More importantly, as can be seen from Figure 3, even the peak current increases from 242 to 481 mA mg^{-1} after 32 sweeps, whereas the proton adsorption/desorption area (the area between −0.2 and 0.0 V vs. SCE) related to the surface of the Pt particles is almost constant, which implies that the enhancement in activity originates from the hydrous ruthenium oxide formed in PtRu/Vulcan during cycling. We infer that the RuO_2·0.56H_2O component in the PtRuO_2·0.56H_2O/CNT catalyst leads to the reduced activation period and thus to a direct advantage for methanol oxidation. In addition, we also note that the peak potentials for the PtRu/Vulcan catalyst get higher and higher during cycling, which indicates the poorer and poorer electronic conductivity and kinetic characteristics of this catalyst. This can be explained by the low mass transport characteristics and electron conductivity of RuO_2·$x$$H_2O$ relative to PtRu alloy in PtRu/Vulcan owing to the compact microstructure of the former.

As shown in Figure 4, significant differences in the onset potential for CO oxidation between the catalysts containing ruthenium and those of pure platinum are observed, thus illustrating the beneficial role of ruthenium for CO oxidation. Comparison of the CO oxidation curves for the ruthenium-containing catalysts (Figures 4a and c) reveals that the onset

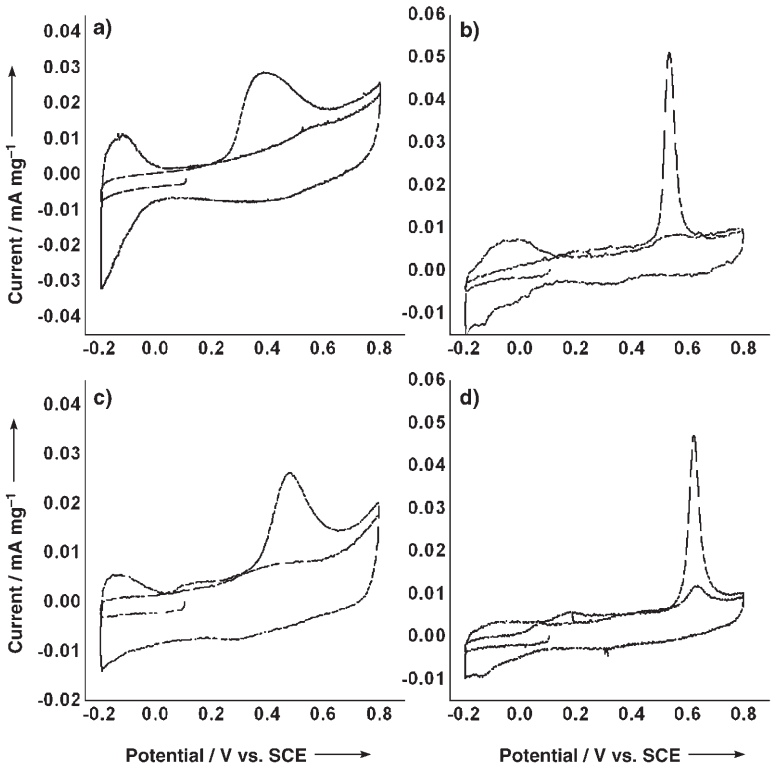

Figure 4. The oxidation of pre-adsorbed CO at 25 °C as measured by CO stripping voltammetry in 1 M $HClO_4$ solution in the potential range −0.2 to 0.8 V vs. SCE at a scan rate of 10 mVs^{-1}: a) PtRuO_2·0.56H_2O/CNT, b) Pt/CNT, c) PtRu/Vulcan, and d) Pt/Vulcan in 1 M $HClO_4$.

potential for $Pt/RuO_2{\cdot}0.56H_2O/CNT$ is found at even lower potential (223 mV) than that of PtRu/Vulcan (338 mV). This demonstrates that although the ruthenium is present as a hydrous ruthenium oxide phase rather than being alloyed, CO oxidation is promoted even more efficiently, as is also underlined by the higher peak current and the broader peak shape.

Dmowski and co-workers[16] have reported that hydrous ruthenium oxide is, in fact, a nanocomposite consisting of dispersed rutile-like nanocrystals the grain boundaries of which are filled with water. The rutile part of $RuO_2{\cdot}xH_2O$ supports electronic conduction, while the hydrous grain-boundary regions are responsible for the proton transport. Another proposed mechanism is that $RuO_2{\cdot}xH_2O$ can dissociate H_2O. The strength of CO adsorption on the surface of RuO_2 is comparable to that of the bond of the bridging O atoms and unlike that on the metallic Ru surface, where bonding of the O atoms is too strong to allow reaction with CO.[18] Therefore, $RuO_2{\cdot}0.56H_2O$ can easily donate hydroxide species to platinum sites to aid CO oxidation, which leads to the excellent catalytic activity observed. Additionally, the corrected surface areas for Pt of the $Pt/RuO_2{\cdot}0.56H_2O/CNT$ and PtRu/Vulcan catalysts are 90.6 and 63.2 m^2g^{-1}, respectively, assuming that CO adsorption occurs only on Pt. This is another reason why $Pt/RuO_2{\cdot}0.56H_2O/CNT$ shows high activity.

In summary, a $Pt/RuO_2{\cdot}0.56H_2O/CNT$ catalyst has been prepared that shows superb performance for direct methanol electrooxidation. The active material of the catalyst, namely Pt and $RuO_2{\cdot}0.56H_2O$, is deposited in a highly dispersed form on the carbon nanotubes owing to the efficient utilization of their huge specific surface area in combination with the slow Pt reduction and Ru^{3+} oxidation during synthesis. We found that the use of CNTs can improve the microstructure of the electrode and facilitate mass transport, thereby increasing the power output. In addition, the $RuO_2{\cdot}0.56H_2O$ coating can directly donate and accept protons as well as electrons within a short timeframe and therefore supply activated Ru^{III}–OH species for removing strongly adsorbed CO from active Pt sites in an oxygen-transfer step, which results in a lower electrode potential for CO oxidation. Moreover, our studies also testify that the CNTs can compensate the loss of electron conductivity caused by the $RuO_2{\cdot}0.56H_2O$ coating, probably by improving the electrode microstructure because of their rigid structure and lowering the resistance of the electrode. This plays an important role in improving the kinetic characteristics and therefore reveals the suitability of Pt decorated on hydrous RuO_2 with appropriate water content for methanol electrooxidation—it is even more active than the PtRu alloy.

Experimental Section

In the first step, CNTs (0.1 g), coated with sodium dodecyl sulfate, were dissolved in a solution of $RuCl_3$ (0.854 mmol) in water (150 mL) by sonication for 5 min. Then, the pH value was adjusted to 4 by adding sodium hydroxide and appropriate amounts of hydrogen peroxide solution. For the platinum deposition step, the as-prepared $RuO_2{\cdot}xH_2O/CNT$ was added to 50 mL of ethylene glycol with constant stirring for 10 min. Then, 410 μL of 0.2 M $H_2[PtCl_6]$ was added with constant stirring. The resulting slurry was refluxed at 140 °C for 3 h to ensure complete reduction of $H_2[PtCl_6]$. The solid product was then rinsed repeatedly with deionized water. Finally, the product was dried in vacuo at 70 °C for 10 h. The catalyst thus obtained is referred to as $Pt/RuO_2{\cdot}xH_2O/CNT$. Pt particles were also deposited on pure CNTs by the same method without the $RuO_2{\cdot}xH_2O$ deposition step (referred to as Pt/CNT) for comparison. TGA and DSC gave an x value of 0.56 for $Pt/RuO_2{\cdot}xH_2O/CNT$. ICP was used to analyze the Ru and Pt content of the samples; the Pt content was 14.8%, with a Pt:Ru atomic ratio of close to 1:1, which indicates only a small loss of Pt and Ru.

Structural catalyst characterization was carried out by X-ray diffraction (XRD; STOE-STADI P, Ge-monochromated $Cu_{K\alpha}$ radiation) and TEM (Philips CM20, W cathode, 200 kV acceleration voltage). Electrochemical measurements were carried out at 25 °C in a three-electrode cell connected to a Solartron workstation. A gold patch (1×1 cm^2) coated with catalyst ink was used as the working electrode. A saturated calomel electrode (SCE) and Pt gauze were used as reference and counter electrodes, respectively. A solution of 1 M $CH_3OH + 1$ M $HClO_4$ was used as electrolyte. All the reagents used were of analytical grade. Several activation scans were performed until reproducible voltammograms were obtained. Cyclic voltammograms were recorded in the potential range −0.2 to 0.8 V vs. SCE at a scan rate of 50 $mV\,s^{-1}$. Only the last cycles were used for comparison of the catalytic activity of the specified catalysts. The oxidation of pre-adsorbed CO was measured by CO stripping voltammetry in 1 M $HClO_4$ solution at a scan rate of 10 $mV\,s^{-1}$. All the recorded currents are corrected for the weight percentage of the platinum in catalysts.

Received: April 3, 2006
Published online: July 17, 2006

Keywords: fuel cells · methanol · nanotubes · platinum · ruthenium

[1] K. Kordesch, G. Simader, *Fuel Cells and their Applications*, Wiley-VCH, Weinheim, **1996**.
[2] T. S. Ahmadi, Z. L. Wang, T. C. Green, A. Henglein, M. A. El-Sayed, *Science* **1996**, *272*, 1924–1926.
[3] H. P. Liang, H. M. Zhang, J. S. Hu, Y. G. Guo, L. J. Wan, C. L. Bai, *Angew. Chem.* **2004**, *116*, 1566–1569; *Angew. Chem. Int. Ed.* **2004**, *43*, 1540–1543.
[4] H. Wakayama, N. Setoyama, Y. Fukushima, *Adv. Mater.* **2003**, *15*, 742–745.
[5] M. Watanabe, S. Motoo, *J. Electroanal. Chem.* **1975**, *60*, 267–272.
[6] X. M. Ren, P. Zelenay, S. Thomas, J. Davey, S. Gottesfeld, *J. Power Sources* **2000**, *86*, 111–116.
[7] F. Maillard, E. R. Savinova, P. A. Simonov, V. I. Zaikovskii, U. Stimming, *J. Phys. Chem. B* **2004**, *108*, 17893–17904.
[8] M. Arenz, K. J. J. Mayrhofer, V. Stamenkovic, B. B. Blizanac, T. Tomoyuki, P. N. Ross, N. M. Markovic, *J. Am. Chem. Soc.* **2005**, *127*, 6819–6829.
[9] F. Maillard, G. Q. Lu, A. Wieckowski, U. Stimming, *J. Phys. Chem. B* **2005**, *109*, 16230–16243.
[10] Z. G. Chen, X. P. Qiu, B. Lu, S. C. Zhang, W. T. Zhu, L. Q. Chen, *Electrochem. Commun.* **2005**, *7*, 593–596.
[11] H. A. Gasteiger, N. Markovic, P. N. Ross, E. J. Cairns, *J. Phys. Chem. B* **1994**, *97*, 12020–12029.
[12] A. Kabbabi, R. Faure, R. Durand, B. Beden, F. Hahn, J. M. Leger, C. Lamy, *J. Electroanal. Chem.* **1998**, *444*, 41–53.
[13] A. Hamnett, *Catal. Today* **1997**, *38*, 445–457.
[14] D. R. Rolison, P. L. Hagans, K. E. Swider, J. W. Long, *Langmuir* **1999**, *15*, 774–779.

[15] J. W. Long, R. M. Stroud, K. E. Swider-Lyons, D. R. Rolison, *J. Phys. Chem. B* **2004**, *108*, 9772 – 9776.
[16] W. Dmowski, T. Egami, K. E. Swider-Lyons, C. T. Love, D. R. Rolison, *J. Phys. Chem. B* **2002**, *106*, 12677 – 12683.
[17] W. H. Lizcano-Valbuena, V. A. Paganin, E. R. Gonzalez, *Eleotrochim. Acta* **2002**, *47*, 3715 – 3722; M. Watanabe, M. Uchida, S. Motoo, *J. Electroanal. Chem.* **1987**, *229*, 395..
[18] H. Over, Y. D. Kim, A. P. Seitsonen, S. Wendt, E. Lundgren, M. Schmid, P. Varga, A. Morgante, G. Ertl, *Science* **2000**, *287*, 1474 – 1476.

